

# Direct determination of the ionization energies of FeO and CuO with VUV radiation

Ricardo B. Metz<sup>a)</sup>*Department of Chemistry, University of Massachusetts Amherst, Amherst, Massachusetts 01003*

Christophe Nicolas and Musahid Ahmed

*Chemical Sciences Division, Lawrence Berkeley National Laboratory, Berkeley, California 94720*

Stephen R. Leone

*Departments of Chemistry and Physics and Lawrence Berkeley National Laboratory, University of California, Berkeley, California 94720*

(Received 23 June 2005; accepted 18 July 2005; published online 22 September 2005)

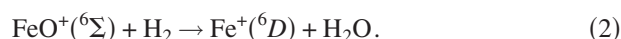
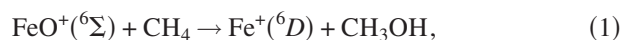
Photoionization efficiency curves were measured for gas-phase FeO and CuO using tunable vacuum-ultraviolet radiation at the Advanced Light Source. The molecules are prepared using laser ablation of a metal-oxide powder in a novel high-repetition-rate source and are thermally moderated in a supersonic expansion. These measurements provide the first directly measured ionization energy for CuO,  $IE(\text{CuO})=9.41\pm 0.01$  eV. The direct measurement also gives a greatly improved ionization energy for FeO,  $IE(\text{FeO})=8.56\pm 0.01$  eV. The ionization energy connects the dissociation energies of the neutral and cation, leading to a refined bond strength for the FeO cation:  $D_0(\text{Fe}^+-\text{O})=3.52\pm 0.02$  eV. A dramatic increase in the photoionization cross section at energies of 0.36 eV above the threshold ionization energy is assigned to autoionization and direct ionization involving one or more low-lying quartet states of  $\text{FeO}^+$ . The interaction between the sextet ground state and low-lying quartet states of  $\text{FeO}^+$  is key to understanding the oxidation of hydrogen and methane by  $\text{FeO}^+$ , and these experiments provide the first experimental observation of the low-lying quartet states of  $\text{FeO}^+$ . © 2005 American Institute of Physics. [DOI: 10.1063/1.2032947]

## INTRODUCTION

Transition-metal oxides are important catalysts commercially and in biology.<sup>1-4</sup> For example, copper oxide and mixed metal oxides containing iron are widely used for alkene oxidation,<sup>1,2,5</sup> and CuO catalyzes methanol synthesis from  $\text{CO}/\text{H}_2$ .<sup>6</sup> Metal-oxide centers are also responsible for the conversion of methane to methanol on iron and copper-doped zeolites.<sup>4,7,8</sup> Biologically, methane mono-oxygenase (MMOs) are enzymes that convert methane to methanol. Soluble MMO has an active di-iron center,<sup>9</sup> while particulate MMO has active copper centers.<sup>10</sup> Studies of the isolated metal oxides (MO) and the cations ( $\text{MO}^+$ ) can aid in revealing the mechanisms and key intermediates of these reactions.<sup>8,11-13</sup>

The isolated FeO is important in the chemistry of the Earth's atmosphere, where it is produced by the rapid reaction of Fe atoms deposited by meteors with ozone.<sup>14,15</sup> In the interstellar medium, shock waves can liberate metal oxides from grains, and FeO has been detected by radioastronomy towards Sagittarius B2 Main.<sup>16,17</sup> Iron-containing compounds are highly efficient flame suppressants, and they are being studied as possible substitutes for ozone-depleting halons.<sup>18</sup> As a result, there have been many studies of the thermodynamics and spectroscopy of transition-metal oxides.<sup>19</sup>

The reactions of transition-metal-oxide cations have also been extensively studied, most notably because of the ability of several gas-phase  $\text{MO}^+$  to convert methane to methanol under thermal conditions.<sup>12,20-22</sup> Calculations predict that, of the first-row transition metals,  $\text{CuO}^+$  would most efficiently convert methane to methanol.<sup>23</sup> This reaction has not been studied experimentally, due to the difficulty of producing  $\text{CuO}^+$ , although  $\text{CuO}^+$  ligated by phenanthroline does convert propane and larger alkanes to alcohols.<sup>24</sup> The reactions of  $\text{FeO}^+$  have received particular attention. The reactions of  $\text{FeO}^+$  with methane and hydrogen are spin allowed:



However, the calculations predict that the minimum-energy pathway for these reactions is through low-spin quartet intermediates. Thus, at thermal energies, these reactions require two spin changes. As a result, although reaction (2) is quite exothermic, it is very inefficient, occurring at 1% of the collision rate. This "two-state reactivity" has been studied extensively by Shaik, Schwarz, and coworkers.<sup>25</sup> Although an understanding of the dynamics of reactions (1) and (2) requires knowledge of the energies of low-lying quartet states of  $\text{FeO}^+$ , as well as their coupling to the sextet ground state, these states have not been previously observed, and electronic structure calculations give inconsistent predictions.

Photoionization studies are carried out here to measure the ionization energies of FeO and CuO. In addition to their

<sup>a)</sup>Author to whom correspondence should be addressed. Electronic mail: rbmetz@chemistry.umass.edu

intrinsic utility, accurate ionization energies (IEs) for the metal oxides lead to improved bond strengths for MO or  $\text{MO}^+$ , since the bond strengths ( $D_0$ ) of the neutral and ion are related:

$$D_0(M^+ - \text{O}) - D_0(M - \text{O}) = \text{IE}(M) - \text{IE}(\text{MO}). \quad (3)$$

Photoionization can also provide a means to access interesting low-lying electronic states: for example, photoionization of FeO ( $X, {}^5\Delta_4$ ) can form both the high-spin ground state and low-spin excited states of  $\text{FeO}^+$ . The novel aspect of the experiments here is the marriage of a high-repetition-rate laser-ablation source with a synchrotron light source for tunable ionization studies. This provides access to a wide range of oxide molecules for an accurate determination.

## EXPERIMENT

Literature thermochemistry predicts that one-photon ionization of FeO and CuO requires vacuum-ultraviolet (VUV) light below 142 and 133 nm, respectively.<sup>26,27</sup> These refractory molecules can only be produced in low concentrations in the gas phase. Tunable laboratory VUV sources are often not sufficiently intense to produce sufficient ion signals, while resonant two-color, two-photon ionization (1 + 1' REMPI) is problematic due to the low dissociation energies and extremely complex spectroscopy of the neutrals.<sup>19</sup> As a result, the experiments are performed at the Chemical Dynamics Beamline located at the Advanced Light Source (ALS) at Lawrence Berkeley National Laboratory. The laser-ablation photoionization spectrometer is described elsewhere,<sup>28</sup> so only modifications required for the study of the metal oxides are discussed here in detail.

The ALS produces tunable VUV radiation in pulses separated by 2 ns. Each pulse of the ablation laser produces an  $\sim 40\text{-}\mu\text{s}$  packet of the metal and metal oxide, so the challenge is to couple a pulsed laser-ablation source to an effectively continuous light source. This is accomplished by operating the laser-ablation source at a high repetition rate,<sup>29</sup> using a Nd:YLF laser running at 1 kHz. In earlier photoionization studies at the beamline, we produced vanadium oxides by Nd:YAG laser ablation (at 100 Hz) of a vanadium rod followed by reaction with  $\text{O}_2$ . This method is impractical for FeO and CuO for two reasons. The late transition metals bind oxygen much less strongly than the early metals in the series, so reactions of Fe or Cu with noncorrosive precursors such as oxygen and  $\text{N}_2\text{O}$  are endothermic or prohibitively slow near thermal energies,<sup>30</sup> although they have been observed in ablation sources.<sup>31,32</sup> Second, the 1-kHz Nd:YLF laser produces  $\sim 160\text{-ns}$  pulses, significantly longer than the  $\sim 5\text{-ns}$  pulses of the Nd:YAG laser. As a result, yields of metal oxides are very low.

These difficulties are solved by using a pressed powder of the metal oxide itself as an ablation target. For CuO, a rod of pressed copper (II) oxide was ground in a ball mill and compressed into a 8.4-mm-diameter,  $\sim 25\text{-mm}$ -long rod with an isostatic low-temperature press. For FeO, powdered  $\text{Fe}_3\text{O}_4$  is mixed with 20% by weight graphite, since pure  $\text{Fe}_3\text{O}_4$  pressed rods crumbled. Rods were glued to an aluminum support and mounted to a rotating, translating control-

ler. Each rod could be used for several hours ( $>10^7$  laser pulses). Atoms and molecules formed by ablation are entrained and thermally moderated in a gas pulse from a piezoelectric pulsed valve<sup>33</sup> using helium or oxygen at  $\sim 2$  atm (1 atm = 101.3 kPa) backing pressure. Ions are deflected out of the molecular beam, before the skimmer, by a set of deflection plates. Tunable VUV light crosses the neutral molecular beam 9 cm downstream of the rotating rod, in the extraction region of a Wiley-McLaren time-of-flight mass spectrometer. Photoions are extracted with a high-voltage pulse and are collected on a microchannel plate detector. Ion time-of-flight spectra are collected with a multichannel scalar card. Typical signal levels are 0.01  $\text{FeO}^+$  ions/laser pulse. The measured photoion yields allow us to estimate the concentration of Fe and FeO in the interaction region:  $6 \times 10^8$  and  $2 \times 10^8 \text{ cm}^{-3}$ , respectively. These values are based on the absolute photoionization cross section of atomic Fe,  $5.0 \times 10^{-18} \text{ cm}^2$  at 8.05 eV (Ref. 34) and the relative cross section measured by Tondello at higher energies.<sup>35</sup> The photoionization cross section of FeO has not been measured, but is assumed to be the same as that of Fe ( $7 \times 10^{-18} \text{ cm}^2$ ) near 10 eV, a region well above the threshold and free of resonances.

Bernstein and coworkers have used Nd:YAG laser ablation of a metal foil, followed by reaction with oxygen, to produce neutral  $\text{Fe}_m\text{O}_n$  and  $\text{Cu}_m\text{O}_n$  clusters.<sup>31,32</sup> Clusters were detected following 118-nm (10.5-eV) photoionization. Also, the ablation of CuO pellets produces a wide range of  $\text{Cu}_m\text{O}_n$  neutral<sup>31</sup> and ionic<sup>36</sup> clusters. However, our source appears to only produce bare metal and diatomic metal oxides; no larger metal-containing molecules are detected, even at ionization photon energies above 11 eV. This is likely due to the longer Nd:YLF pulse resulting in a more gentle ablation. Also, our ablation source works in the free-rod mode (the molecular beam is not constrained in a channel), so clustering is minimized. The ablation of pressed powders should also provide a convenient way to prepare other refractive species such as metal carbides and nitrides.

Photoionization efficiency curves are measured by integrating either the  ${}^{56}\text{FeO}^+$  or the  ${}^{63}\text{CuO}^+ + {}^{65}\text{CuO}^+$  signal and normalizing it to photon flux. For the survey scans, the photon flux was measured using a NIST-calibrated Si photodiode. The energy scale was calibrated, and the linewidth of the VUV light was determined with the aid of autoionizing resonances in atomic copper,<sup>37,38</sup> iron,<sup>35</sup> and xenon.<sup>39</sup> The light from an undulator at the ALS is spectrally dispersed with a 3-m monochromator, resulting in approximately  $10^{13}$  photons/s. Survey scans use a 600- $\mu\text{m}$  slit in the 3-m monochromator, providing a 15-meV linewidth near 8.7 eV and 35 meV near 12.5 eV; a 200- $\mu\text{m}$  slit is used for scans near thresholds, resulting in a 6-meV linewidth near 8.7 eV.

## RESULTS AND DISCUSSION

### Photoionization of FeO

Figure 1 shows survey photoionization efficiency (PIE) curves for FeO in helium and oxygen carrier gas. The use of an oxygen carrier leads to better vibrational and electronic cooling of FeO, as evidenced by the lack of ionization below

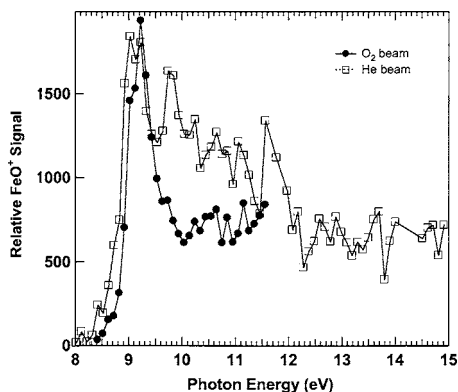


FIG. 1. Survey photoionization efficiency curves of  $^{56}\text{FeO}$  in helium carrier gas (dashed lines) and oxygen carrier gas (solid lines). Data points are spaced by 100 meV. Improved thermal moderation by oxygen leads to a higher energy onset and to sharper features in the spectrum.

8.5 eV and a sharper onset near 8.9 eV in Fig. 1. However, interference in the mass spectrum due to the photoionization of  $\text{O}_2$  limits scans in oxygen to energies below 11.7 eV. Nevertheless, all data are obtained using oxygen as the carrier gas. The survey spectrum of FeO in  $\text{O}_2$  shows a small onset near 8.5 eV, followed by a plateau and a much larger onset near 8.9 eV. Figure 2(a) shows a PIE curve for FeO in the region of the ionization onset. The sharpness of the onset and very low ion signals at lower energies provide evidence for effective vibrational and electronic cooling by the  $\text{O}_2$  carrier gas. The onset is sharp and occurs at  $\text{IE}(\text{FeO}) = 8.56 \pm 0.01$  eV. The ground states of FeO and  $\text{FeO}^+$  are well characterized and can explain the sharp onset of ionization. FeO has a  $^5\Delta_4$  ground state with  $r_0 = 1.619$  Å, as measured by optical and microwave spectroscopy.<sup>19,40–42</sup> The resonance-enhanced photodissociation electronic spectra<sup>43</sup> of  $\text{FeO}^+$  show that its ground state is  $^6\Sigma$ , with  $r_0 = 1.643$  Å. Because it has no orbital angular momentum, this state has no first-order spin-orbit splitting. Because the bond lengths of the neutral and ion are very similar, the photoionization onset of FeO ( $X, ^5\Delta_4$ ) to  $\text{FeO}^+(X, ^6\Sigma)$  should be sharp, as is observed. Our value of the ionization energy of FeO slightly revises the best previous direct measurement by Hildenbrand, who obtained  $8.71 \pm 0.10$  eV based on the electron impact ionization efficiency of FeO using Fe as a reference.<sup>26</sup>

The bond strength of neutral FeO has been measured by several groups (Table I).<sup>14,26,44–48</sup> The classic technique is to measure equilibria between Fe, FeO, and  $\text{FeO}_2$  (and O and  $\text{O}_2$ ) at a high temperature using mass spectrometry. The difficulty lies in extrapolating measurements over an  $\sim 400$ -K range near 2000 K to low temperatures. Recently, Chestakov *et al.* determined  $D_0(\text{Fe}-\text{O}) = 4.18 \pm 0.01$  eV by using velocity map imaging to measure the kinetic energy of Fe ( $^5D$ ) following the photodissociation of FeO.<sup>48</sup> This value is consistent with the earlier measurements but is significantly more precise.

Armentrout and co-workers have measured the  $\text{FeO}^+$  bond strength using the endothermic reactions of  $\text{Fe}^+$  with  $\text{O}_2$  and ethylene oxide in a guided ion-beam spectrometer, obtaining  $D_0(\text{Fe}^+-\text{O}) = 3.47 \pm 0.06$  eV.<sup>49,50</sup> The observation of predissociation of the  $v' = 0$  level of an excited  $^6\Sigma$  state of

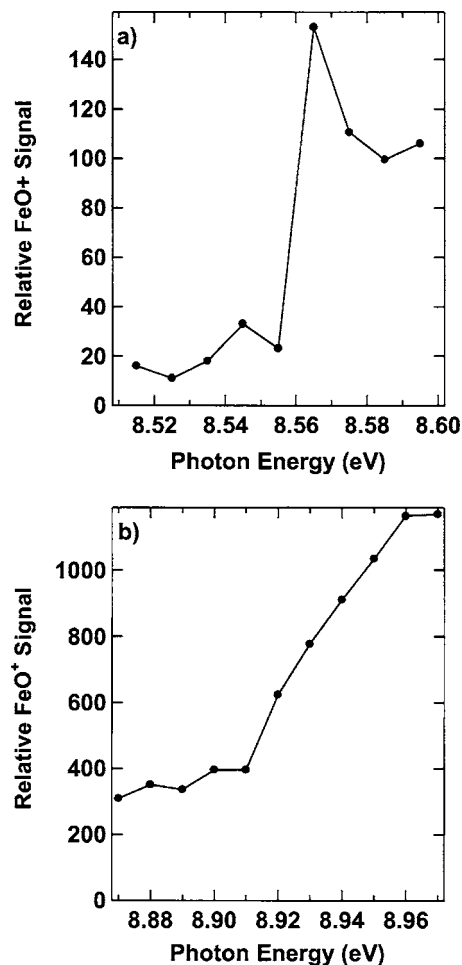


FIG. 2. Photoionization efficiency curves for  $^{56}\text{FeO}$  in oxygen carrier gas showing (a) the ionization onset at  $8.56 \pm 0.01$  eV and (b) a second onset at 8.92 eV, 0.36 eV above the ionization energy. Data points are spaced by 10 meV.

$\text{FeO}^+$  places an upper limit on  $D_0(\text{Fe}^+-\text{O})$  of  $\leq 3.552$  eV.<sup>43,51</sup> Our measured ionization energy of FeO and the precise FeO bond strength measured by Chestakov *et al.*<sup>48</sup> allow an independent evaluation of  $D_0(\text{Fe}^+-\text{O})$ :

TABLE I. Measurements of  $D_0$  (0 K) of FeO.

$D_0(\text{FeO})$ (eV)	Method
$4.21 \pm 0.13$	Equilibrium (high $T$ ) <sup>a</sup>
$4.17 \pm 0.08$	Equilibrium (high $T$ ) <sup>b</sup>
$4.20 \pm 0.13$	Equilibrium (high $T$ ) <sup>c</sup>
$4.03 \pm 0.13^d$	Equilibrium (high $T$ ) <sup>c</sup>
$4.16 \pm 0.08$	Equilibrium (high $T$ ) <sup>f</sup>
$4.18 \pm 0.01$	Photofragment imaging <sup>g</sup>
$4.13 \pm 0.06$	$D_0(\text{Fe}^+-\text{O})^h$ and $\text{IE}(\text{FeO})^i$

<sup>a</sup>Reference 44.

<sup>b</sup>Reference 45.

<sup>c</sup>Reference 26.

<sup>d</sup>This value has been revised to  $4.16 \pm 0.08$  eV (Ref. 14).

<sup>e</sup>Reference 46.

<sup>f</sup>Reference 47.

<sup>g</sup>Reference 48.

<sup>h</sup>References 49 and 50.

<sup>i</sup>This work.

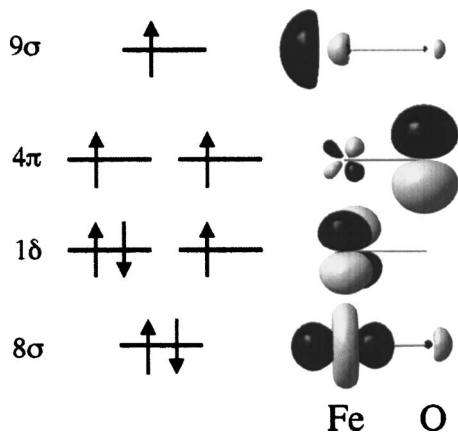


FIG. 3. Low-lying molecular orbitals and electron occupancy of FeO ( $X, {}^5\Delta$ ).

$$D_0(\text{Fe}^+ - \text{O}) = D_0(\text{Fe} - \text{O}) - \text{IE}(\text{FeO}) + \text{IE}(\text{Fe}). \quad (4)$$

Using  $\text{IE}(\text{Fe}) = 7.9024$  eV (Ref. 52) gives  $D_0(\text{Fe}^+ - \text{O}) = 3.52 \pm 0.02$  eV. This result agrees with and refines the guided ion-beam value.

The photoionization yield of FeO also rises dramatically near 8.92 eV, as shown in Fig. 1 and, in a finer scan, in Fig. 2(b). Unlike the first onset, which was sharp, this second onset is relatively gradual, occurring over  $\sim 40$  meV. Above 9.2 eV, the photoionization efficiency decreases, reaching a plateau at  $\sim 9.8$  eV. The plateau is most likely due to direct ionization to one or more excited states of  $\text{FeO}^+$ , while the enhanced signal near 9.1 eV is likely due to resonances from autoionizing Rydberg states that have a  $\text{FeO}^+$  excited-state core. Figure 3 shows the electron occupancy and molecular orbitals of FeO ( $X, {}^5\Delta$ ). Orbitals are calculated here at the MP2/6-311+G( $d,p$ ) level using GAUSSIAN.<sup>53</sup> Photoionization by removal of an electron with  $s = -1/2$  from the non-bonding  $1\delta$  orbital produces the  ${}^6\Sigma$  ground state of  $\text{FeO}^+$ . Several low-lying quartet states of  $\text{FeO}^+$  can be formed by removing an electron from the  $9\sigma$ ,  $4\pi$ , or  $1\delta$  orbitals. Table II shows the energies of these states, as calculated by several groups.<sup>20,23,54,55</sup> Although different levels of theory give different energy orderings for the quartet states, the calculations consistently predict several low-lying quartet states with similar energies, lying 0.25–1.5 eV above the ground sextet state. Excited sextet states lie at higher energy, as they in-

volve removing an electron from low-lying orbitals such as the  $3\pi$  orbital.<sup>43</sup> The second onset that we observe at an energy of  $\geq 0.36$  eV above the ionization energy is thus most likely due to the autoionization of Rydberg states with a  $\text{FeO}^+$  (quartet) core and to direct ionization to quartet states of  $\text{FeO}^+$ . The gradual onset is likely due to accessing several autoionizing states, as well as to direct ionization to multiple spin-orbit states and possibly multiple electronic states of  $\text{FeO}^+$ . For comparison, the spin-orbit splitting in FeO ( $X, {}^5\Delta$ ) is 23 meV,<sup>19</sup> and the spin-orbit splitting in the  ${}^6\Pi$  excited state of  $\text{FeO}^+$  is 8 meV.<sup>43</sup> The photoelectron spectrum of FeO would give the positions of these low-lying states of  $\text{FeO}^+$ , along with spin-orbit and, possibly, vibrational spacings; thus photoelectron imaging experiments are planned.

The excited electronic states of metal-containing atoms frequently have dramatically different reactivities from the ground state.<sup>25,56</sup> This is also likely to be the case for  $\text{FeO}^+$ . The oxidation of hydrogen and methane by ground state  $\text{FeO}^+$  is spin allowed, since  $\text{FeO}^+$  and  $\text{Fe}^+$  have sextet ground states. However, the barriers on the sextet potential-energy surface are higher than on the low-spin quartet surface, so at thermal energies, the reaction involves two spin changes (sextet  $\rightarrow$  quartet  $\rightarrow$  sextet).<sup>57,58</sup> This “two-state reactivity” sequence is thought to lead to a low efficiency in the exothermic conversion of  $\text{H}_2$  to  $\text{H}_2\text{O}$  by  $\text{FeO}^+$ .<sup>25</sup> The reaction of the low-lying, low-spin quartet state of  $\text{FeO}^+$  should be much more efficient—it would require one fewer spin change to produce sextet  $\text{Fe}^+$ , and the lowest quartet state of  $\text{Fe}^+$  is energetically accessible at 0.23 eV. The photoionization of FeO at 9.8 eV provides a means to produce primarily quartet  $\text{FeO}^+$  for subsequent reaction studies.

### Photoionization of CuO

Figure 4 shows a survey photoionization efficiency spectrum for CuO; the inset shows a fine scan in the threshold region. The photoionization onset is sharp, and there is no evidence for additional thresholds at higher energy. The sharpness is also well understood from the geometries of CuO and  $\text{CuO}^+$ . From the onset, the ionization energy of CuO is deduced to be  $9.41 \pm 0.01$  eV. The ground and low-lying excited states of CuO have been extensively studied.<sup>19</sup> The ground state is  ${}^2\Pi_{3/2}$ , with the outer electronic configuration  $\dots(8\sigma^2)(1\delta^2)(9\sigma^2)(4\pi^3)$  and  $r_0 = 1.729$  Å.<sup>59–62</sup> Bond-

TABLE II. Calculated energies (eV) of electronic states of  $\text{FeO}^+$  formed by photoionization of FeO ( $X, {}^5\Delta$ ).

Electron removed	$\text{FeO}^+$ state	Level of theory				
		NLSD <sup>a</sup>	CASPT <sup>b</sup>	QCISD(T) <sup>b</sup>	B3LYP <sup>c</sup>	MR-SDCI <sup>d</sup>
$-1\delta$	${}^6\Sigma$	0.0	0.0	0.0	0.0	0.0
$-4\pi$	${}^4\Phi$	1.1	0.8	0.57		0.54
$-1\delta$	$2\ {}^4\Delta$	1.4				
$-1\delta$	${}^4\Gamma$	1.3				
$-9\sigma$	$1\ {}^4\Delta$	1.0			0.25	0.89
$-4\pi$	${}^4\Pi$					0.54

<sup>a</sup>Reference 20.

<sup>b</sup>Reference 54.

<sup>c</sup>Reference 23.

<sup>d</sup>Reference 55.

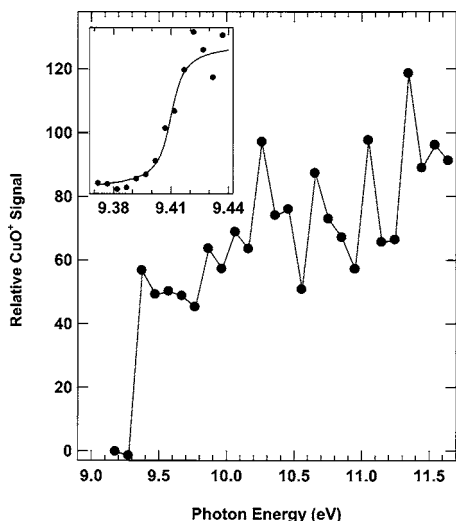


FIG. 4. Survey photoionization efficiency curve of CuO in oxygen carrier gas (dashed lines). Data points are separated by 100 meV. The inset shows the photoionization efficiency curve near the ionization threshold, with data points taken every 5 meV. The solid line is a sigmoid with the instrumental resolution centered at the ionization onset of  $9.41 \pm 0.01$  eV.

ing in this state is predominantly ionic, arising from  $\text{Cu}^+(3d^{10})-\text{O}^-(2s^2 2p^5)$ . The  $^3\Sigma$  ground state of  $\text{CuO}^+$  is formed by removing an electron from the  $4\pi$  orbital, which is primarily an oxygen  $2p_{\pi}$  and is weakly antibonding. This state is calculated<sup>12,20,55,62</sup> to have a bond length of 1.68–1.76 Å.  $\text{CuO}^+(X, ^3\Sigma)$  and  $\text{CuO}(X, ^2\Pi_{3/2})$  have similar bond lengths, and the ground state of  $\text{CuO}^+$  does not have spin-orbit splitting, so the photoionization onset should be sharp, as is observed.

The best values for  $D_0(\text{Cu}-\text{O})$  and  $D_0(\text{Cu}^+-\text{O})$  are from guided ion-beam studies by Rodgers *et al.*,<sup>27</sup> who looked at the reactions of  $\text{Cu}^+$  with  $\text{O}_2$ ,  $\text{CO}$ ,  $\text{CO}_2$ ,  $\text{N}_2$ ,  $\text{NO}$ ,  $\text{N}_2\text{O}$ , and  $\text{NO}_2$ . Many of the reactions do not occur efficiently at the thermodynamic onset, since the ground state of  $\text{Cu}^+$  is  $3d^{10}(^1S)$ . The onsets for reactions with  $\text{NO}_2$  to yield  $\text{CuO} + \text{NO}^+$  and  $\text{CuO}^+ + \text{NO}$  gave  $D_0(\text{Cu}-\text{O}) = 2.94 \pm 0.12$  eV and  $D_0(\text{Cu}^+-\text{O}) = 1.35 \pm 0.12$  eV, respectively. From the difference between these onsets, and the well-known ionization energy of  $\text{NO}$ , the authors obtain  $\text{IE}(\text{CuO}) = 9.34 \pm 0.06$  eV. This is consistent with our direct measurement of  $\text{IE}(\text{CuO}) = 9.41 \pm 0.01$  eV. Thus, our measurement supports the current values of  $D_0(\text{Cu}-\text{O})$  and  $D_0(\text{Cu}^+-\text{O})$ .

## CONCLUSIONS

We developed a high-repetition-rate laser-ablation source to produce beams of refractory materials. Using this source, we measured the photoionization efficiency curves for FeO and CuO, obtaining  $\text{IE}(\text{FeO}) = 8.56 \pm 0.01$  eV and  $\text{IE}(\text{CuO}) = 9.41 \pm 0.01$  eV. Combining the ionization energy with the dissociation energy<sup>48</sup> of FeO gives an improved value of  $D_0(\text{Fe}^+-\text{O}) = 3.52 \pm 0.02$  eV. A dramatic increase in the photoionization cross section near 8.92 eV is most likely due to autoionization and direct ionization involving low-lying quartet states of  $\text{FeO}^+$ .

## ACKNOWLEDGMENTS

The authors gratefully thank James Wu (Materials Science Division, Lawrence Berkeley Laboratory) for making the pressed metal-oxide rods and Dr. Kevin R. Wilson (Chemical Sciences Division, Lawrence Berkeley Laboratory) for assistance with the experiment. R.B.M. acknowledges financial support from the National Science Foundation under Grant No. CHE-0308439. This work was supported by the Director of the Office of Energy Research, Office of Basic Energy Sciences, Chemical Sciences Division of the U.S. Department of Energy under Contract No. DE-AC02-05CH11231.

- <sup>1</sup>D. J. Hucknall, *Selective Oxidation of Hydrocarbons* (Academic, London, 1974).
- <sup>2</sup>G. Centi, F. Cavani, and F. Trifirò, *Selective Oxidation by Heterogeneous Catalysis* (Kluwer, New York, 2001).
- <sup>3</sup>*Metal-Oxo and Metal-Peroxo Species in Catalytic Oxidations* Struct. Bonding (Berlin) **97** (2000).
- <sup>4</sup>A. E. Shilov and A. A. Shteinman, *Acc. Chem. Res.* **32**, 763 (1999).
- <sup>5</sup>J. B. Reitz and E. I. Solomon, *J. Am. Chem. Soc.* **120**, 11467 (1998).
- <sup>6</sup>Z. Y. Ma, C. Yang, W. Wei, W. H. Li, and Y. H. Sun, *J. Mol. Catal. A: Chem.* **231**, 75 (2005).
- <sup>7</sup>R. Raja and P. Ratnasamy, *Appl. Catal., A* **158**, L7 (1997).
- <sup>8</sup>K. Yoshizawa, Y. Shiota, T. Yumura, and T. Yamabe, *J. Phys. Chem. B* **104**, 734 (2000).
- <sup>9</sup>A. C. Rosenzweig, C. A. Frederick, S. J. Lippard, and P. Nordlund, *Nature (London)* **366**, 537 (1993).
- <sup>10</sup>R. L. Lieberman and A. C. Rosenzweig, *Nature (London)* **434**, 177 (2005).
- <sup>11</sup>K. Yoshizawa, *J. Inorg. Biochem.* **78**, 23 (2000).
- <sup>12</sup>D. Schröder, H. Schwarz, and S. Shaik, *Struct. Bonding (Berlin)* **97**, 91 (2000).
- <sup>13</sup>K. A. Zemski, D. R. Justes, and A. W. Castleman, Jr., *J. Phys. Chem. B* **106**, 6136 (2002).
- <sup>14</sup>R. J. Rollason and J. M. C. Plane, *Phys. Chem. Chem. Phys.* **2**, 2335 (2000).
- <sup>15</sup>W. J. McNeil, R. A. Dressler, and E. Murad, *J. Geophys. Res., [Space Phys]* **106**, 10447 (2001).
- <sup>16</sup>C. M. Walmsley, R. Bachiller, G. P. les Forêts, and P. Schilke, *Astrophys. J.* **566**, L109 (2002).
- <sup>17</sup>R. S. Furuya, C. M. Walmsley, K. Nakanishi, P. Schilke, and R. Bachiller, *Astron. Astrophys.* **409**, L21 (2003).
- <sup>18</sup>C. B. Kellogg and K. K. Irikura, *J. Phys. Chem. A* **103**, 1150 (1999).
- <sup>19</sup>A. J. Merer, *Annu. Rev. Phys. Chem.* **40**, 407 (1989).
- <sup>20</sup>A. Fiedler, D. Schröder, S. Shaik, and H. Schwarz, *J. Am. Chem. Soc.* **116**, 10734 (1994).
- <sup>21</sup>D. Schröder and H. Schwarz, *Angew. Chem., Int. Ed. Engl.* **34**, 1973 (1995).
- <sup>22</sup>D. K. Böhme and H. Schwarz, *Angew. Chem., Int. Ed.* **44**, 2336 (2005).
- <sup>23</sup>Y. Shiota and K. Yoshizawa, *J. Am. Chem. Soc.* **122**, 12317 (2000).
- <sup>24</sup>D. Schröder, M. C. Holthausen, and H. Schwarz, *J. Phys. Chem. B* **108**, 14407 (2004).
- <sup>25</sup>D. Schröder, S. Shaik, and H. Schwarz, *Acc. Chem. Res.* **33**, 139 (2000).
- <sup>26</sup>D. L. Hildenbrand, *Chem. Phys. Lett.* **34**, 352 (1975).
- <sup>27</sup>M. T. Rodgers, B. Walker, and P. B. Armentrout, *Int. J. Mass. Spectrom.* **183**, 99 (1999).
- <sup>28</sup>C. Nicolas, J. Shu, D. S. Peterka, L. Poisson, S. R. Leone, and M. Ahmed, *J. Chem. Phys.* (to be submitted).
- <sup>29</sup>M. Smits, C. A. de Lange, S. Ullrich, T. Schultz, M. Schmitt, J. G. Underwood, J. P. Shaffer, D. M. Rayner, and A. Stolow, *Rev. Sci. Instrum.* **74**, 4812 (2003).
- <sup>30</sup>J. M. C. Plane and R. J. Rollason, *J. Chem. Soc., Faraday Trans.* **92**, 4371 (1996).
- <sup>31</sup>Y. Matsuda, D. N. Shin, and E. R. Bernstein, *J. Chem. Phys.* **120**, 4165 (2004).
- <sup>32</sup>D. N. Shin, Y. Matsuda, and E. R. Bernstein, *J. Chem. Phys.* **120**, 4157 (2004).
- <sup>33</sup>D. Proch and T. Trickl, *Rev. Sci. Instrum.* **60**, 713 (1989).
- <sup>34</sup>G. G. Lombardi, P. L. Smith, and W. H. Parkinson, *Phys. Rev. A* **18**,

- 2131 (1978).
- <sup>35</sup>G. Tondello, *Mem. Soc. Astron. Ital.* **46**, 113 (1975).
- <sup>36</sup>J. R. Gord, R. J. Bemish, and B. S. Freiser, *Int. J. Mass Spectrom. Ion Processes* **102**, 115 (1990).
- <sup>37</sup>M. Müller, M. Schmidt, and P. Zimmermann, *Europhys. Lett.* **2**, 359 (1986).
- <sup>38</sup>M. A. Baig, M. Hanif, S. A. Bhatti, and J. Hormes, *J. Phys. B* **30**, 5381 (1997).
- <sup>39</sup>A. Kortyna, M. R. Darrach, P.-T. Howe, and A. Chutjian, *J. Opt. Soc. Am. B* **17**, 1934 (2000).
- <sup>40</sup>A. S. C. Cheung, R. M. Gordon, and A. J. Merer, *J. Mol. Spectrosc.* **87**, 289 (1981).
- <sup>41</sup>T. Krockertskothén, H. Knockel, and E. Tiemann, *Mol. Phys.* **62**, 1031 (1987).
- <sup>42</sup>M. D. Allen, L. M. Ziurys, and J. M. Brown, *Chem. Phys. Lett.* **257**, 130 (1996).
- <sup>43</sup>F. Aguirre, J. Husband, C. J. Thompson, K. L. Stringer, and R. B. Metz, *J. Chem. Phys.* **119**, 10194 (2003).
- <sup>44</sup>G. Balducci, G. De Maria, M. Guido, and V. Piacente, *J. Chem. Phys.* **55**, 2596 (1971).
- <sup>45</sup>D. E. Jensen and G. A. Jones, *J. Chem. Soc., Faraday Trans. 1* **69**, 1448 (1973).
- <sup>46</sup>E. Murad, *J. Chem. Phys.* **73**, 1381 (1980).
- <sup>47</sup>S. Smoes and J. Drowart, *High. Temp. Sci.* **17**, 31 (1984).
- <sup>48</sup>D. A. Chestakov, D. H. Parker, and A. V. Baklanov, *J. Chem. Phys.* **122**, 084302 (2005).
- <sup>49</sup>S. K. Loh, E. R. Fisher, L. Lian, R. H. Schultz, and P. B. Armentrout, *J. Phys. Chem.* **93**, 3159 (1989).
- <sup>50</sup>P. B. Armentrout and B. L. Kicketl, *Organometallic Ion Chemistry*, edited by B. S. Freiser (Kluwer, Dordrecht, The Netherlands, 1994).
- <sup>51</sup>J. Husband, F. Aguirre, P. Ferguson, and R. B. Metz, *J. Chem. Phys.* **111**, 1433 (1999).
- <sup>52</sup>J. Sugar and C. Corliss, *J. Phys. Chem. Ref. Data* **14**, 1 (1985).
- <sup>53</sup>M. J. Frisch, G. W. Trucks, H. B. Schlegel *et al.*, GAUSSIAN98, Revision A.3, Gaussian, Inc., Pittsburgh, PA, 1998.
- <sup>54</sup>A. Fiedler, J. Hrusák, W. Koch, and H. Schwarz, *Chem. Phys. Lett.* **211**, 242 (1993).
- <sup>55</sup>Y. Nakao, K. Hirao, and T. Taketsugu, *J. Chem. Phys.* **114**, 7935 (2001).
- <sup>56</sup>P. B. Armentrout, *Annu. Rev. Phys. Chem.* **41**, 313 (1990).
- <sup>57</sup>D. Schröder, H. Schwarz, D. E. Clemmer, Y. Chen, P. B. Armentrout, V. Baranov, and D. K. Bohme, *Int. J. Mass Spectrom. Ion Processes* **161**, 175 (1997).
- <sup>58</sup>Y. Shiota and K. Yoshizawa, *J. Chem. Phys.* **118**, 5872 (2003).
- <sup>59</sup>O. Appelblad and A. Lagerqvist, *Can. J. Phys.* **53**, 2221 (1975).
- <sup>60</sup>M. C. L. Gerry, A. J. Merer, U. Sassenberg, and T. C. Steimle, *J. Chem. Phys.* **86**, 4754 (1987).
- <sup>61</sup>H. Xian, Z. X. Cao, X. Xu, X. Lu, and Q. E. Zhang, *Chem. Phys. Lett.* **326**, 485 (2000).
- <sup>62</sup>D. Hippe and S. D. Peyerimhoff, *Mol. Phys.* **76**, 293 (1992).